A missing piece of the *Papio* puzzle: Gorongosa baboon phenostructure and intrageneric relationships

Felipe I. Martinez [a, *], Cristian Capelli [b], Maria J. Ferreira da Silva [c, d], Vera Aldeias [e, f], Zeresenay Alemseged [g], William Archer [f, q], Marion Bamford [h], Dora Biro [b], René Bobe [e, i, j], David R. Braun [k], Jörg M. Habermann [e, i, l], Tina Lüdecke [i, m], Hilário Madiquida [n], Jacinto Mathe [j], Enquye Negash [k], Luis M. Paulo [o], Maria Pinto [o], Marc Stalmans [j], Frederico Tátá [e, o], Susana Carvalho [e, i, j, p]

[a] Pontificia Universidad Católica de Chile, Facultad de Ciencias Sociales, Programa de Antropología, Av. Vicuña Mackenna 4860, Macul, Santiago 7820436, Chile
[b] Department of Zoology, University of Oxford, UK
[c] Organisms and Environment Division, School of Biosciences, Cardiff University, Biomedical Sciences Building, Room C/5.15, Museum Avenue, Cardiff CF10 3AX, Wales, UK
[d] CIBIO/InBio, Centro de Investigação em Biodiversidade e Recursos Genéticos, Universidade do Porto, Portugal
[e] ICArEHB — Interdisciplinary Center for Archaeology and Evolution of Human Behaviour, University of Algarve, Campus de Gambelas, 8005-139 Faro, Portugal
[f] Department of Human Evolution, Max Planck Institute for Evolutionary Anthropology, Leipzig, Germany
[g] Department of Organismal Biology & Anatomy, University of Chicago, USA
[h] Evolutionary Studies Institute, University of the Witwatersrand, South Africa
[i] Primate Models for Behavioural Evolution Lab, Institute of Cognitive and Evolutionary Anthropology, School of Anthropology and Museum Ethnography, University of Oxford, UK
[j] Gorongosa National Park, Sofala, Mozambique
[k] Center for the Advanced Study of Human Paleobiology, George Washington University, 800 22nd Street NW, Washington DC 20052, USA
[l] GeoZentrumNordbayern, Friedrich-Alexander-Universität Erlangen-Nürnberg, Germany
[m] Senckenberg Biodiversity and Climate Research Centre, Germany
[n] Universidade Eduardo Mondlane, Maputo, Mozambique
[o] AESDA — Associação de Estudos Subterrâneos e Defesado Ambiente, Portugal
[p] Centre for Functional Ecology, Coimbra University, Portugal
[q] Department of Archaeology, University of Cape Town, Cape Town, South Africa

A R T I C L E   I N F O

A B S T R A C T

Most authors recognize six baboon species: hamadryas (*Papio hamadryas*), Guinea (*Papio papio*), olive (*Papio anubis*), yellow (*Papio cynocephalus*), chacma (*Papio ursinus*), and Kinda (*Papio kindae*). However, there is still debate regarding the taxonomic status, phylogenetic relationships, and the amount of gene flow occurring between species. Here, we present ongoing research on baboon morphological diversity in Gorongosa National Park (GNP), located in central Mozambique, south of the Zambezi River, at the southern end of the East African Rift System. The park exhibits outstanding ecological diversity and hosts more than 200 baboon troops. Gorongosa National Park baboons have previously been classified as chacma baboons (*P. ursinus*). In accordance with this, two mtDNA samples from the park have been placed in the same mtDNA clade as the northern chacma baboons. However, GNP baboons exhibit morphological features common in yellow baboons (e.g., yellow fur color), suggesting that parapatric gene flow between chacma and yellow baboons might have occurred in the past or could be ongoing. We investigated the phenostructure of the Gorongosa baboons using two approaches: 1) description of external phenotypic features, such as coloration and body size, and 2) 3D geometric morphometric analysis of 43 craniofacial landmarks on 11 specimens from Gorongosa compared to a pan-African sample of 352 baboons. The results show that Gorongosa baboons exhibit a mosaic of features shared with southern *P. cynocephalus* and *P. ursinus griseipes*. The GNP baboon phenotype fits within a

geographic clinal pattern of replacing allotaxa. We put forward the hypothesis of either past and/or ongoing hybridization between the gray-footed chacma and southern yellow baboons in Gorongosa or an isolation-by-distance scenario in which the GNP baboons are geographically and morphologically intermediate. These two scenarios are not mutually exclusive. We highlight the potential of baboons as a useful model to understand speciation and hybridization in early human evolution.

1. Introduction

Baboons (*Papio* spp.) are distributed across sub-Saharan Africa and a small part of the Arabian Peninsula. Five baboon morphotypes have usually been recognized as full-rank phylogenetic species (Newman et al., 2004; Zinner et al., 2009; Keller et al., 2010; Kopp et al., 2015; see Fig. 1): hamadryas (*Papio hamadryas*), Guinea (*Papio papio*), olive (*Papio anubis*), yellow (*Papio cynocephalus*), and chacma baboons (*Papio ursinus*). In the 2016 IUCN assessment, the Kinda baboon (*Papio kindae*), previously considered a subspecies of the yellow baboon (*Papio cynocephalus kindae*), was upgraded to full species status. However, there is still debate regarding the taxonomic status of baboon morphotypes, their phylogenetic relationships, and the amount of hybridization occurring between them. Several hybrid zones between baboon morphotypes have been identified (e.g., Awash River, Ethiopia [Phillips-Conroy and Jolly, 1986]; Amboseli, Kenya [Samuels and Altmann, 1986]; Kafue National Park, Zambia [Jolly et al., 2011]), suggesting that gene flow has been the norm rather than the exception within the genus *Papio*. One supposed boundary between species is central Mozambique (Kingdon, 1997; Zinner et al., 2009), a region poorly investigated so far. In this paper, we focus on this area by providing the first morphological description of the baboons in Gorongosa National Park (GNP), located in central Mozambique, just a few kilometers away from the boundary between yellow and chacma baboons (Fig. 2).
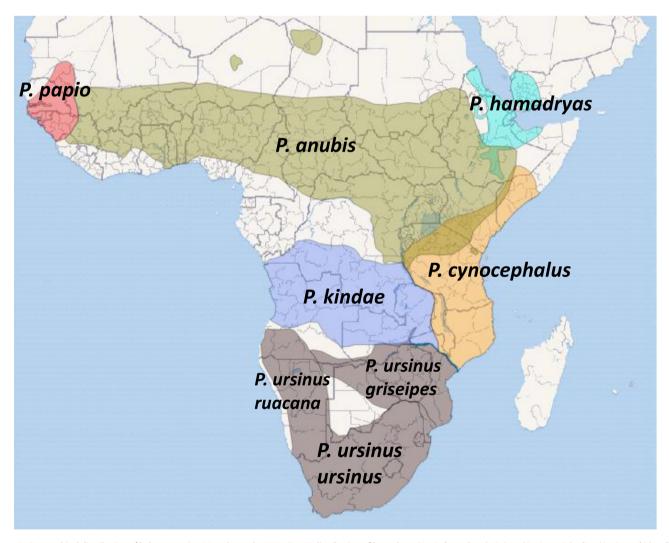

Figure 1. Geographical distribution of baboon species. Map shows the IUCN (2017) distribution of hamadryas (*Papio hamadryas*), Guinea (*Papio papio*), olive (*Papio anubis*), yellow (*Papio cynocephalus*), Kinda (*Papio kindae*) and chacma baboons (*Papio ursinus*). Map also shows the distribution of subspecies grayfooted chacma (*Papio ursinus griseipes*), Cape chacma (*P. ursinus ursinus*) and ruacana chacma baboons (*Papio ursinus ruacana*).
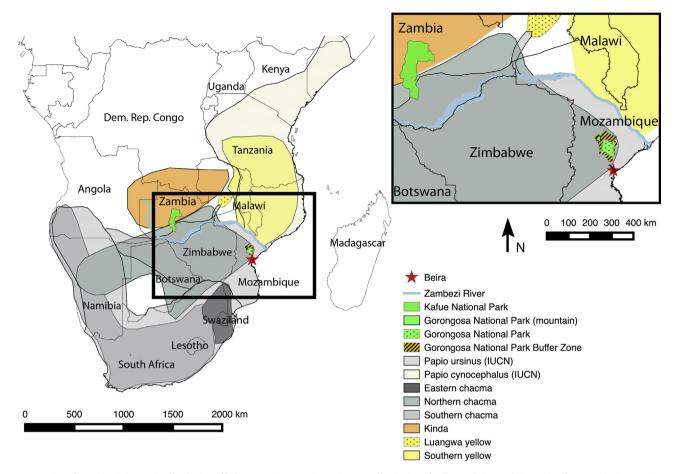
Figure 2. Location of GNP in relation to the distribution of baboon species. Map shows the IUCN distribution of yellow and chacma baboons (Hoffmann and Hilton-Taylor, 2008; Kingdon et al., 2016) and the distribution of Luangwa yellow, southern yellow, eastern chacma, northern chacma and southern chacma as estimated by Keller et al. (2010) using mitochondrial DNA sequence information. Genetic evidence for hybridization between Kinda and grayfooted chacma has been observed in Kafue National Park (central Zambia; Jolly et al., 2011). In Luangwa National Park (east Zambia) yellow and grayfooted chacma live in close proximity (Burrell, 2009). The Lower Zambezi River is most likely a boundary between grayfooted chacma and yellow baboons.

The six-species taxonomy is based on the phylogenetic species concept (PSC; Cracraft, 1983; Jolly, 2001), which emphasizes diagnosable aspects of the phenotype and monophyly to distinguish between taxa. By contrast, under the biological species concept (BSC; Dobzhansky, 1937; Mayr, 1942, 1982), *Papio* morphotypes would be considered subspecies of a single polytypic species (Jolly, 1993). Several authors have asserted that the evidence of natural hybridization makes the BSC taxonomic nomenclature of subspecies more suitable for *Papio* morphotypes (Frost et al., 2003; Barrett and Henzi, 2008; Singleton et al., 2017). However, under the BSC nomenclature, geographically-circumscribed diversity would be underappreciated, due in part to the limitations of the Linnaean system (Jolly, 2003; Burrell, 2009). To avoid this inconsistency between the PSC and BSC definitions, Jolly (2001) uses the term allotaxa (Grubb, 1999) to describe baboon variation. Jolly (2001: 193—194) defines allotaxa as "phylogenetically close, but well-differentiated and diagnosable geographically replacing forms whose ranges do not overlap, but are either disjunct, adjoining, or separated by comparatively narrow zones in which characters are clinally distributed".

It has long been recognized that *Papio* species are morphologically well-differentiated (Kingdon, 1997) and parapatrically distributed (Jolly, 1993, 2001). This observation is mainly based on diagnostic features of the phenotype, such as fur color and texture, body build, skull morphology, or tail carriage. Populations located near contact zones often exhibit mixed characteristics, making them intermediate forms. For example, Ibean yellow baboons from Kenya and Somalia display physical characteristics from olive baboons (Jolly, 1993). Also according to Jolly (1993), yellow baboons from Zambia, Malawi, and northern Mozambique were in the past mistakenly classified as chacma baboons (*P. ursinus jubilaeus* and "dwarf chacma"; Jolly, 1993). In Zambia, the yellow baboons from Luangwa National Park are currently classified as *P. cynocephalus jubilaeus*, and their mitochondrial DNA (mtDNA) haplotype is found in baboons at the Senga Hills Forest Reserve in Malawi (Zinner et al., 2015). In north-central Mozambique, yellow baboons are sometimes referred as *P. cynocephalus jubilaeus*, *P. cynocephalus strepitus*, or simply *P. cynocephalus* spp., which reflects the lack of taxonomic agreement at the subspecies level in this region (Hill, 1970; Zinner et al., 2015). Thus, it is often interpreted that the external morphological features defining *Papio* species change in a stepwise regional pattern.

Previous morphometric studies have characterized baboon morphotype differences in craniofacial shape and sexual dimorphism as related to size and allometric scaling (Leigh and Cheverud, 1991; Collard and O'Higgins, 2001; Singleton, 2002; Frost et al., 2003; Leigh, 2006; Singleton et al., 2017). There is agreement that most of the cranial shape variation seen in *Papio* is explained by allometric scaling, with only *P. kindae* departing from a common ontogenetic trajectory (Leigh, 2006; Singleton et al., 2017). In addition, *Papio* craniofacial variation across geography has been modeled as a continuous northwest—southeast cline (Frost et al.,

2003; Dunn et al., 2013). Frost et al. (2003) found that geographic location explains 60% of the variation in craniofacial shape after correcting for size and sex. Dunn et al. (2013) corroborated this finding, but added an east to west pattern of increasing and then decreasing size with no evidence of a Bergmannian trend. In addition, their study could not find any ecological correlation between cranial morphology and environmental variables such as temperature, humidity, precipitation, vegetation, and altitude, with the exception of a correlation between centroid size and precipitation standard deviation in olive baboons. Although ecological factors (food resources, seasonality) cannot be ruled out (Dunbar, 1990), the morphometric data seem to favor population history and isolation by distance as straightforward explanations to the above-mentioned continental trend in craniofacial variation (Frost et al., 2003; Dunn et al., 2013).

The *Papio* northwest—southeast phenotypic cline includes a break that creates a north—south dichotomy between *P. papio*, *P. hamadryas*, and *P. anubis* in the north and *P. cynocephalus*, *P. kindae*, and *P. ursinus* in the south (Frost et al., 2003; Jolly, 2003). The differences between north and south translate morphologically into northern morphotypes exhibiting a broader cranium and face than the narrower midface of the southern morphotypes. Also, southern morphotypes have a more downwardly flexed face relative to the braincase (increased klinorhynchy), producing a taller midface (Frost et al., 2003; Singleton et al., 2017). This north—south dichotomy is also reflected in pelage features: "wavy, bushy shoulder manes and cheek tufts" in the north and "straight, silky mane hairs, untufted cheeks and light facial patches" in the south (Jolly, 2003:1046).

The genetic data are also consistent with the north/south division. The most complete phylogenetic analyses carried out for *Papio* sp. (Zinner et al., 2009, 2011a,b, 2013, 2015) replicated the north—south dichotomy but also revealed discordance between mtDNA phylogeny and morphology. Zinner et al. (2009) analyzed mtDNA variation in 67 specimens at 53 sites and identified seven main mtDNA haplogroups (labeled A—G) divided into two major geographic clades—a southern clade, grouping together *P. ursinus*, *P. kindae*, and southern *P. cynocephalus* (A—C; Zinner et al., 2009), and a northern clade, including *P. hamadryas*, *P. papio*, *P. anubis*, and northern *P. cynocephalus* (haplogroups D—G). The mismatch between yellow baboon morphotype and mitochondrial grouping indicates that *P. cynocephalus* is mitochondrially paraphyletic. This suggests a complex evolutionary history with several episodes of gene flow leading to different degrees of introgressive hybridization (Zinner et al., 2009, 2013; Keller et al., 2010).

Based on mtDNA data, southern *P. cynocephalus* are grouped into the same haplogroup (B) as the northern *P. ursinus*. Keller et al. (2010) further investigated the southern mtDNA subclades with an emphasis on geographically close areas and suggested that males from the *P. ursinus* morphotype introgressed the southern *P. cynocephalus* range from south to north. As a result of this process, the southern *P. cynocephalus* populations maintained their yellow baboon mtDNA but acquired a mixed or predominantly chacma morphotype (via nuclear swamping: Burrell, 2009; Zinner et al., 2009, 2011a,b; Keller et al., 2010). Although alternative explanations could be drawn (such as lineage sorting), this scenario is in agreement with the female philopatry and male dispersal exhibited by *P. ursinus* and *P. cynocephalus* (Barrett and Henzi, 2008; Fischer et al., 2017). It also fits the pattern of mtDNA subclade paraphyly between northern and southern *P. ursinus* and may explain the difficulty in assigning the baboons found in Malawi and eastern Zambia (*P. c. (u.) jubilaeus*), and north-central Mozambique (*P. c. jubilaeus* and *P. c. strepitus*) to the described morphotypes (Jolly, 1993). In turn, it predicts a morphological cline between *P. ursinus griseipes* (grayfooted chacma) and southern

P. cynocephalus (through regionally replacing allotaxa) and the occurrence of further hybridization in contact zones north to the Middle Zambezi River (see Jolly et al., 2011). *Papio u. griseipes* has gray feet, and a lighter coat color, longer tail, slightly smaller cranium, and larger body size than *P. ursinus ursinus* (Jolly, 1993; Burrell, 2009). The distribution of the grayfooted chacma ranges from south-central Mozambique to the extreme north of South Africa, Zimbabwe, north Botswana, south Zambia, a small portion of the extreme southeast of Angola, and a small portion of the extreme northeast of Namibia (see Sithaldeen et al., 2009), including the Caprivi strip (Fig. 1). According to Zinner et al. (2009) and Keller et al. (2010), the distribution of the northern chacma subclade most likely coincides with the subspecies *P. ursinus griseipes* (grayfooted chacma).

In Mozambique, the Lower Zambezi River is considered a biogeographic barrier between *P. cynocephalus* and *P. ursinus* (Kingdon, 1997). However, *P. u. griseipes* populations extend north over the Upper or Middle Zambezi River to the northeast and hybridize with *P. kindae* in the Kafue Valley in Zambia (Jolly et al., 2011). In fact, Jolly et al. (2011) found groups with individuals carrying mtDNA and Y chromosomes from both the Kinda and grayfooted chacma baboons, suggesting hybridization between these two parental species. Jolly et al. (2011) also studied phenotypic features exhibited in hybrid individuals, detecting troops with different degrees of genetic admixture and intermediate morphotypes. In addition to this, *P. u. griseipes* populations are in contact with *P. cynocephalus* in the lower Luangwa Valley in Zambia (Burrell, 2009). Although it is yet unclear how far east this contact persists, Burrell (2009) argues the contact likely extends, north of the Zambezi, to the Indian Ocean in the Mozambican coast.

In this study, we set out to place the morphological variation of the baboon population in GNP within the context of broader regional diversity. The Gorongosa baboons were identified as chacma baboons in an earlier study (Tinley, 1977) and were more recently placed within the geographic range of the northern chacma mtDNA clade (Zinner et al., 2009; Keller et al., 2010; see figure 2). However, the Gorongosa baboons exhibit some features common to the yellow baboon, such as yellow fur, lightly-colored ventral hair, pink infraorbital skin, and other features frequently seen in the grayfooted chacma baboon, such as robust male body build, bent tail carriage, or downwardly flexed facial orientation (Figs. 3 and 4). These observations lead to the hypothesis that parapatric gene flow between the grayfooted chacma and southern yellow baboons might have occurred in the past or could be currently ongoing in the GNP (Freedman, 1963; Booth and Freedman, 1970; Napier, 1981).

Documenting hybridization in grayfooted chacma baboons and the observed phenostructure of Gorongosa baboon troops is an interesting way to further explore baboon morphological diversity. Phenostructure corresponds to the information about the distribution of heritable traits, functionally intertwined with information about interbreeding or zygostructure (Jolly, 1993, 2003). We first describe the external phenotype of the Gorongosa baboon as compared to *P. u. griseipes*, *P. u. ursinus*, typical *P. cynocephalus*, and *P. kindae*. Second, we comparatively analyze Gorongosa baboon craniofacial morphology by means of geometric morphometric tools and place it within the broader context of *Papio* variation.

2. Materials and methods

2.1. Study area

Gorongosa National Park (total area 3770 km^2) is located in the central/northern part of Mozambique. It is bordered to the south by

Figure 3. (a—j). Images depicting the phenotypic diversity of GNP baboons. Numbers correspond to morphological features described in Table 1. Photographs by various members of the Paleo Primate Project (PPP) team. 1: General fur color, 2: Dorsal coat color, 3: Ventral hair color, 4: Limb color, 5: Eyelid skin color, 6: Circum-orbital skin color, 7: Hand hair color, 8: Presence of silvery fringe on hands, 9: Male body build, 10: Sexual dimorphism, 11: Tail shape, 12: Facial orientation, 13: Natal coat color, 14: Infant stage two hair color.

Figure 4. (a—f). Images depicting the phenotypic diversity of southern Africa baboons. a) Kinda baboons (*P. kindae*) at Kasanka National Park, Zambia (photo by Megan Petersdorf). b) Male yellow baboon (*P. cynocephalus* spp.) at Quirimbas NP, Mozambique (photo by Daniel Cara). c) Male grayfooted chacma (*P. ursinus griseipes* or *P. ursinus chobiensis*) at Chobe NP, Botswana (photo by Michael Haworth). d) Female Cape chacma baboons (*P. ursinus ursinus*) at Cape Peninsula (photo by Maria J. Ferrerira da Silva). e) Male grayfooted chacma (*P. ursinus griseipes*) at Okavango Delta, Botswana (photo by John Weir). f) Male Cape chacma (*P. ursinus ursinus*) at Cape Peninsula (photo by Maria J. Ferrerira da Silva).

the Pungue River and to the north by the Nhandue River, and is located 100 km south of the Zambezi River, a major hydrological feature of the African continent. The park exhibits outstanding biodiversity, with habitats spanning from tall evergreen forests inside limestone gorges to miombo woodlands, to grassy *Acacia* woodlands, tall open *Combretum* woodlands, open floodplain grasslands, and seasonally flooded grasslands.

2.2. Observation of external phenotypic features

To evaluate the degree of morphological variation in GNP baboons, we qualitatively listed the phenotypic characteristics observed in baboons during fieldwork and from field-recorded visual material (photographs and videos). The field season at GNP spanned six weeks, on average, during July—August 2016 and 2017. We used the following techniques to record video, take

photographs, and complete observations: a) systematic follows of non-habituated groups in woodlands, b) surveys across the floodplain and woodlands, and c) close-proximity observations of human-habituated groups at Chitengo Camp.

We listed 14 phenotypic Gorongosa baboon features related to coloration and body size/shape (general fur color, color of dorsal hair, color of ventral hair, color of limbs, eyelid skin color, circumorbital skin color, hand/foot hair color, presence of silvery fringe on hands/feet, male body build, degree of sexual dimorphism, tail shape, facial orientation, natal coat color, infant stage two hair color; see Table 1). We compared these characteristics to the yellow, Kinda, grayfooted chacma, and southern chacma baboon features described in the literature (Altmann et al., 1981; Jolly, 1993; Alberts et al., 2001; Jolly et al., 2011; Swedell, 2011; Chiou, 2018). Infant stage two (estimated age 8—18 months) was defined according to Altmann et al. (1981).

Table 1
External characteristics of GNP baboons compared to yellow and gray-footed chacma baboons.

	Phenotypic feature	Gorongosa baboons	Gray-footed chacma baboons	Southern chacma baboons	Yellow baboons	Kinda baboons
1	General color	Yellow-brown to gray-brown	Gray-brown[a]	Dark-brown[a]	Yellow-brown[a]	Yellow-brown[a]
2	Color of dorsal hair	Yellow-brown to gray-brown	Drab gray-brown[b]	Dark-brown[a]	Yellow-brown[c]	Yellow-brown[a,b]
3	Color of ventral hair	Light yellow	Lighter.[a] Such as back and limbs[b]	Dark. Sometimes lighter than dorsal hair[a]	Light yellow[a,c]	Light yellow[a]
4	Color of limbs	Hindlimbs are lighter than forelimbs	Uniform (in most cases)	Uniform	Uniform (in most cases)	Uniform
5	Eyelid skin color	Pink	Pink	Pink	Pink	Pink
6	Circum-orbital skin color	Some individuals show pink infra-orbital skin	Dark, except pregnant female[b]	Dark	Pink in some populations (e.g. Luangwa, Catapu)	Light pink "spectacles" surrounding eyes[b]
7	Hand/foot hair color	Self (like limbs) in most individuals	Self (like limbs) or gray[a]	Dark[a]	Self (like limbs)[a]	Self (like limbs)[a]
8	Silvery fringe on hands/feet	Present in some individuals	Absent[a]	Absent[a]	Present[a]	Present[a]
9	Male Body build	Robust but some individuals are taller and thinner	Robust[b]	Robust[b]	Taller and thinner.[b] (Robust in *P.c. jubilaeus*).	Very gracile, long limbed[b]
10	Sexual dimorphism	Greater (only observed, not measured)	Greater (adult male 2.0 to 1.9 times adult female)[b,f]	Greater (adult male 2.0 to 1.8 times adult female)[b,e]	Greater to Smaller (adult male 2.1 to 1.6 times adult female)[f]	Smaller (adult male 1.7 to 1.5 times adult female)[b,e]
11	Tail shape	Bent in most individuals; high arch in some females	Bent[a]	Bent[a]	Bent but variable[a]	Arched[a] or usually high arch[b]
12	Facial orientation	Downwardly flexed (increased klinorhynchy)	Downwardly flexed[a] (increased klinorhynchy)	Downwardly flexed[a] (increased klinorhynchy)	"Normal"[a] (less klinorhynchy)	"Normal"[a] (less klinorhynchy)
13	Natal coat	Black	Black[a,b]	Black[a]	Black[a]	White[b]
14	Infant-2[d] hair color	Yellow, lighter than adults. (In transition Infant1-2, black spots in tail and head remain longest).	Brown to cream-colored.	Dark-brown.	Brown to cream-colored, often lighter than adults. (In transition Infant 1−2, black spots in tail and shoulders remain longest).[d]	Brown to cream-colored.[e]

[a] Jolly (1993).
[b] Jolly et al. (2011).
[c] Alberts and Altmann (2001).
[d] Altmann et al. (1981).
[e] Chiou (2018).
[f] Swedell (2011).

2.3. Morphometric sampling and data acquisition

The sample for morphometric analysis comprises 363 cranial specimens (homologous three-dimensional [3D] landmark configurations representing the baboon craniofacial skeleton). Table 2 shows the composition of the morphotypes pursuant to sex and sample size. Our sample combines coordinate data obtained from two different sources: eight baboon skulls from Gorongosa National Park and a comparative sample of 355 baboon skulls from an earlier

Table 2
Morphotypes composition in the morphometric sample (including *P. cynocephalus* geographic subdivision in parentheses).

	Male (*n*)	Female (*n*)	Total (*n*)
Papio anubis	112	43	155
Papio cynocephalus	40	21	61
P. cynocephalus north	(31)	(15)	(46)
P. cynocephalus south	(4)	(2)	(6)
P. cynocephalus DRC	(5)	(4)	(9)
Papio hamadryas	31	8	39
Papio kindae	10	7	17
Papio papio	12	1	13
Papio ursinus	51	12	63
Papio ursinus griseipes	4	0	4
Gorongosa	7	4	11
Total	267	96	363

study conducted by Dunn et al. (2013). The eight baboon skulls from Gorongosa National Park were collected during the 2016 and 2017 fieldwork. The skulls were from naturally deceased and taphonomically-skeletonized individuals. The skulls were surface-scanned in three different views using a NextEngine Desktop 3D Scanner from NextEngine, Inc., operating with both laser and normal light. Each view was a 360° scan with 11 divisions. The geometric point resolution was set to 66 dots per inch (DPI). ScanStudio 2.0.2 software (NextEngine, Inc., 2006) was used to merge the view scans into a single-surface model. Sholts et al. (2011) evaluated the precision of surface models generated by the Next Engine Scanner. Although well-recognized that manually-digitized measurements exhibit better overall precision, surfaces obtained with the Next Engine Scanner are suitable for craniometric research and are comparable to digitized coordinates (Sholts et al., 2011). The surface models were imported into the Amira 5.5 software (Mercury Inc. USA). A set of 43 three-dimensional landmarks was digitized on each baboon craniofacial surface model (see Table 3 for anatomical landmark description). These 43 landmarks were selected from the configuration of landmarks used by Dunn et al. (2013). We selected type I and II landmarks (Bookstein, 1991) to circumvent the differences in measurement error between coordinates obtained with digitizers and the 3D models.

The comparative database corresponds to three hundred and fifty-five specimens with manually digitized coordinates from Dunn et al. (2013). In their database, specimens are grouped into

Table 3
Anatomical definitions of the forty-three, three-dimensional landmarks used in this study.

Landmark number	Description[a]
1	Prosthion: antero-inferior point on projection of pre-maxilla between central incisors
2	Prosthion2: antero-inferior-most point on pre-maxilla, equivalent to prosthion but between central and lateral incisors
3	Anterior-most point of canine alveolus
4	Mesial P3: most mesial point on P3 alveolus, projected onto alveolar margin
5—8	Contact points between adjacent pre-molars/molars, projected labially onto alveolar margin
9	Posterior midpoint onto alveolar margin
10—13	Contact points between adjacent pre-molars/molars, projected lingually onto alveolar margin
14[b]	Anterior-most point of incisive foramen
15[b]	Middle-line point of the incisive foramen projected onto its margin
16	Posterior-most point of incisive foramen
17	Greater palatine foramen
18	Point of maximum curvature on the posterior edge of the palatine
19	Tip of posterior nasal spine
20—21	Anterior and posterior tip of the external auditory meatus
22	Inion: most posterior point of the cranium
23	Asterion: Most lateral meeting point of mastoid part of temporal bone and supraoccipital
24	Nasospinale: inferior-most midline point of piriform aperture
25	Point corresponding to largest width of piriform aperture
26	Meeting point of nasal and pre-maxilla on margin of piriform aperture
27	Rhinion: most anterior midline point on nasals
28	Nasion: midline point on fronto-nasal suture
29	Glabella: most forward projecting midline point of frontals at the level of the supraorbital ridges
30	Supraorbital notch
31	Frontomalare orbitale: where frontozygomatic suture crosses inner orbital rim
32	Zygo-max superior: antero-superior point of zygomaticomaxillary suture taken at orbit rim
33	Center of nasolacrimal foramen (fossa for lacrimal duct)
34	Frontomalare temporale: where frontozygomatic suture crosses lateral edge of zygoma
35	Maximum curvature of anterior upper margin of zygomatic arch
36	Zygo-temp superior: superior point of zygomaticotemporal suture on lateral face of zygomatic arch
37	Zygo-temp inferior: infero-lateral point of zygomaticotemporal suture on lateral face of zygomatic arch
38	Posterior-most point on curvature of anterior margin of zygomatic process of temporal bone
39	Articular tubercule
40	Distal-most point on post-glenoid process
41	Posterior-most point of zygomatic process of temporal bone
42	Bregma: junction of coronal and sagittal sutures
43	Lambda: junction of sagittal and lamboid sutures

[a] Landmark descriptions from Cardini et al. (2007).
[b] Landmarks defined in this study.

one of the six commonly recognized species, with one subspecies identified for four individuals (*P. ursinus griseipes*). The database also included 317 geo-referenced specimens (274 geo-referenced specimens intersect with the 355 specimens labeled by species and sex). We subdivided *P. cynocephalus* into three subgroups by their geographic location: *P. cynocephalus* north (specimens located north of the Ruaha-Rufiji River in Central Tanzania; Zinner et al., 2015), *P. cynocephalus* south (specimens located south of the Ruaha-Rufiji River) and *P. cynocephalus* DRC (specimens located in the southern part of the Democratic Republic of Congo, labeled as *P. cynocephalus* Zaire in the database from Dunn et al., 2013), which is included in the distribution area of Kinda baboons. Two specimens labeled as *P. ursinus* and one specimen labeled as *P. cynocephalus* had geographic coordinates locating their origin in Gorongosa. Therefore, the specimens were divided into 10 groups, taking into account the six-species scheme, the subspecies *P. ursinus griseipes*, the mtDNA paraphyly of *P. cynocephalus* (grouping yellow baboons according to geographic location), and considering Gorongosa as an independent group (see Supplementary Online Material [SOM]).

2.4. Geometric morphometric analysis

Routine geometric morphometrics procedures were used to analyze landmark configuration data. We performed Generalized Procrustes analysis (GPA) superimposition, minimizing the sum of square Euclidian distances between corresponding landmarks; scaling was done using unit centroid size (Bookstein, 1991; Slice, 2001). Principal component analysis (PCA) was used to visualize sample distributions by projecting the multidimensional Procrustes coordinates into a Euclidian tangent space. The PCA ordination makes no assumption about data classification. Rather, it is meant to explore trends by reducing dimensionality into a set of orthogonal (uncorrelated) components (PC). We first ran the overall PCA on all specimens (males and females together) to explore the general trends in the entire sample. In the following analyses, we treated males and females separately.

As a means to investigate the pattern of shape variation that is not related to changes in size, we performed multivariate regression of shape on natural log-transformed centroid size (pooled by species/subspecies groups), for males and females independently. We obtained a "shape score" vector representing variation associated with the size. Multiple permutation tests (1000 rounds) were performed against the null hypothesis of independence between dependent (shape) and independent (size) variables. Residuals from the multivariate regression were treated as "size-corrected" shape coordinates (Drake and Klingenberg, 2008; Klingenberg and Marugán-Lobón, 2013).

Canonical variates analysis (CVA), discriminant function analysis (DFA), and between-groups PCA ordination were used to investigate the extent to which groups differed from one another. To account for unequal group size, we performed DFA for pairs of groups by leave-one-out cross-validations using 1000 permutation rounds (Klingenberg and Monteiro, 2005). To test the reliability of CVA ordinations, we performed between-groups PCA ordination (Mitteroecker and Bookstein, 2011). We calculated the mean

configuration via GPA for each of the ten groups: *P. anubis*, *P. cynocephalus* north, *P. cynocephalus* south, *P. cynocephalus* DRC, *P. hamadryas*, *P. kindae*, *P. papio*, *P. ursinus*, *P. ursinus griseipes*, and Gorongosa. The CVA, DFA, and between-groups PCA were performed for males and females independently. Female CVA and DFA did not include *P. papio* ($n = 1$) and *P. cynocephalus south* ($n = 2$) due to low sample size, and *P. ursinus griseipes* due to lack of cases. Female between-groups PCA ordination did not include *P. papio* and *P. ursinus griseipes*. All of the procedures were performed using MorphoJ version 1.06d (Klingenberg, 2011). Scatterplots were computed in R (R Core Team).

Finally, we subjected the group mean configurations to a new GPA and computed dendrograms for morphological affinity using UPGMA and Ward's method as recommended for morphometric data (Hammer and Harper, 2008; Püschel et al., 2017). Euclidean distances were used as a similarity index. All principal components (PCs) were used to compute the dendrograms in Past 3.18 software. In order to control for scanning error, we also computed comparative trees excluding the component (PC3) that summarized most differences between the Gorongosa consensus and all other mean configurations in males and females.

2.5. Mantel correlograms

To evaluate the strength of the population history signal in our morphometric dataset, we compared the geographic pattern of phenetic autocorrelation in our data to an empirical model of genetic autocorrelation. To do so, we used Mantel correlograms pursuant to Le Boulengé et al. (1996), Borcard and Legendre (2012), and Diniz-Filho et al. (2013). Mantel correlograms are an extension of the Mantel test. Although the use of Mantel tests in ecology and evolutionary biology has recently been criticized (see Guillot and Rousset, 2013), Mantel correlograms have acceptable power in the absence of equivalent methods for assessing multivariate spatial correlation (Borcard and Legendre, 2012; Legendre et al., 2015). Mantel correlograms evaluate the spatial autocorrelation at different distance classes, computing a correlogram for multivariate data using the Mantel statistic (rM) for each distance class (Legendre and Legendre, 1998). Each distance class included all pairs of points located at a specific distance range from each other. Thus, a correlation index is calculated for each distance class. In our implementation, we used specimen distances instead of population distances. This has two advantages. First, our autocorrelation analysis is blind in relation to species, subspecies, morphotypes, or any group designation, preventing the bias that could result from species misidentification. Second, it increases sample size in order to assure that enough pairs of specimens within a given distance class are compared, which provides a reliable estimate for each rM class. The number of distance classes was set to six in both correlograms to reflect distance intervals closer to 1000 km (1109 km for the genetic correlogram, 1153 km for the overall phenetic correlogram, 1141 km for the male phenetic correlogram, and 1125 km for the female phenetic correlogram). The statistical significance of each distance class was tested by setting 999 permutations. The progressive Bonferroni correction was used to account for multiple testing (Legendre and Legendre, 1998).

Phenetic autocorrelation was computed as morphological distances bounded within non-overlapping intervals of geographic distances. This was computed for the entire geo-referenced dataset ($n = 325$), and separately for males ($n = 241$) and females ($n = 84$). The morphological distances correspond to craniofacial shape distance matrices for each specimen ($n = 325$) calculated based on the Procrustes shape coordinates, centroid size, and "size-corrected" shape residuals. The geographic distance matrix was calculated in km, computing geodesic distances from the geographic coordinates

available for each specimen. Similarly, genetic autocorrelation was computed as genetic distances bounded within non-overlapping intervals of geographic distances. Genetic distances were computed as pairwise distances from a set of publicly available mitochondrial cytochrome b (CYT-B) gene sequences (Zinner et al., 2009; Keller et al., 2010). The sequences ($n = 153$; 1140 base pairs) were geo-referenced and a geodesic distance matrix was calculated in km. Genetic pairwise distances were computed after performing a likelihood ratio test to decide on the best-fit model for nucleotide evolution. Distance matrices and Mantel correlograms were computed in R (R Core Team) using the following packages: ade4 (Dray and Dufour, 2007), ape (Paradis et al., 2004), fossil (Vavrek, 2011), mpmcorrelogram (Matesanz et al., 2011), phangorn (Schliep, 2011), and vegan (Oksanen et al., 2018).

2.6. Surface warping

In order to visualize the shape differences across groups, we computed targeted surface warpings. We obtained a warped surface for the consensus of each PCA ordination by warping one scanned specimen from Gorongosa (No. 34) using the Amira 5.5 software (Mercury Inc. USA) and the Bookstein spline interpolation method (Stalling et al., 2005). To represent female morphology, we followed a similar procedure using a surface obtained from Morphosource (http://morphosource.org/) an online repository of 3D scan data (Copes et al., 2016). This ply surface model corresponds to *P. kindae* specimen with catalog number NHMUK-ZD-1961.776 from the Natural History Museum, London. From each consensus, we targeted warped-surfaces along the principal components using the Evan toolbox (v.1.52, by the European Virtual Anthropology Network-Society www.evan-society.org).

3. Results

3.1. External phenotypic features of the Gorongosa baboon

The GNP baboons exhibit unusual phenotypic diversity, combining some features of the yellow baboon (yellow hair, light ventral hair, pink circum-orbital skin [Fig. 4b], also large male body size as in *P. c. jubilaeus* [Fig. 5a], and silvery fringes in hands and feet as in *P. c. strepitus*), and Kinda baboon (yellow hair, light ventral hair, pink circum-orbital skin; Fig. 4a) with others from the gray-footed chacma baboon (gray-brown hair, large body size, downwardly flexed face; Fig. 4c, e and Fig. 5c). The GNP baboon fur coloration generally varies between yellow-brown and gray-brown, and is paler ventrally, with white inner surfaces of limbs and white patches on the lateral muzzle between the eyes and the nostrils (Fig. 3a–j). Their hindlimbs tend to be paler (yellow) than their forelimbs (yellow-brown). The face is black and the skin around the callosities gray. They have pink eyelid skin (Fig. 3d), and some individuals exhibit pink infraorbital skin (Fig. 3e–f). The facial skeleton points downward (Fig. 3g–j, and Fig. 5b) and the tip of the nose points forward in some females (Fig. 3a). Occasionally, females have a nuchal crest of longer flank hairs.

Adult males have no mane. They have elongated hair tufts along the nape (Figs. 3g and 5b), and some show wavy, dark and bright stripes of hair on the back with long leg hair (Fig. 3f). Sexual dimorphism is considerable (Fig. 3i–j), and sexes seem to show variation in color (i.e., bigger males are darker gray-brown and females are paler yellow-brown). We observed some adult males with yellow fur and sometimes a more slender body build (Fig. 3h). In most individuals, the color of the hands and feet is similar to their corresponding limbs but darker hands and feet were observed in some individuals (Fig. 3e and i). Furthermore, some, but not all, individuals display a silvery fringe on the hands and feet (Fig. 3d

Figure 5. (a—c). Images depicting the mixed characteristics of an adult male baboon from Gorongosa compared to baboons from Malawi and Zimbabwe: a) Yellow baboon (*P. cynocephalus jubilaeus*) at Senga Hills Forest Reserve, Malawi (photo by Jim Auburn). b) Gorongosa baboon (photo by Susana Carvalho). c) Grayfooted chacma (*P. ursinus griseipes*) at Cecil Kop Nature Reserve, Eastern Zimbabwe, located 200 km west of Gorongosa (photo by Marion Bamford). The face points downward in Gorongosa (b) and grayfooted chacma baboons from Zimbabwe (c), but not in Senga Hills Forest Reserve baboon (a). The color of their hands and feet is similar to their arms in Senga Hills Forest Reserve (a) and Gorongosa (b), but not in grayfooted chacma baboons from Zimbabwe (c).

and f). Both, curved and bent/broken tails are present in the population. In broken tails, one-fourth of the tail ascends before descending sharply as if broken, as in the chacma (Fig. 5c). Sometimes, the tail has two breaks (Fig. 3g—h), although this feature could be due to proximate life events, such as fights and wounds. Observed females have a curved tail, sometimes with high-arched tail carriage (Fig. 3i). The natal coat of infants is black and turns completely yellow at infant stage-2; black spots on the tail and head are the last to turn yellow (Fig. 3a—c).

3.2. Principal component analysis before size-correction

Figure 6 shows the distribution pattern of the morphometric data using PCA before correcting for centroid size. Principal component 1 explains the largest amount of variation (45.6%), which is more than four times the variance explained by PC 2 (9.9%). As expected, the variation summarized by PC1 is highly correlated with log-transformed centroid size ($R^2 = 0.9$; $p < 0.0001$)
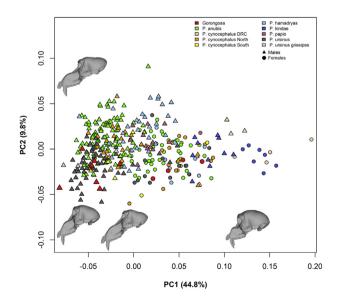

Figure 6. Principal component plot before size correction. Triangles represent males; circles represent females; colors correspond to groups. The shape changes along principal component (PC)1 (45.6% variance) correspond to an increase/decrease in the projection of the face relative to the braincase. The shape changes along the PC2 (9.9% variance) correspond to an increase/decrease in klinorhynchy (downwardly flexed face).

and related to sexual dimorphism (*t*-statistics = 15.21; df = 361; $p < 0.0001$). The first PC differentiates between males and females almost irrespective of species grouping, and shows the degree of sexual dimorphism present in *Papio*. The shape variation along PC1 corresponds to an increase in the projection of the face (facial length and molar row position) relative to the braincase (Fig. 6; PC1, negative end of the distribution), and a decrease in the projection of the face relative to the braincase (Fig. 6; PC1, positive end of the distribution). The shape variation along PC2 corresponds to an increase in klinorhynchy (downwardly flexed face; Fig. 6, PC2, negative end of the distribution) and a decrease in klinorhynchy (Fig. 6; PC2, positive end of the distribution). The PC1—PC2 scatterplot (Fig. 6) shows the distribution of species along a continuum. Larger species, such as *P. ursinus*, *P. anubis* and *P. cynocephalus* (north and south), tend to concentrate towards the negative end of the distribution, whereas the medium-sized *P. papio* and *P. hamadryas* are intermediate. The smaller *P. kindae* falls together with specimens labeled as *P. cynocephalus* from DRC near the positive end of the distribution. An extreme outlier related to PC1 corresponds to a very small individual (ID 2362, see SOM).

3.3. Multivariate regression on size

The regression score resulting from the pooled-within-groups multivariate regression of Procrustes coordinates on natural log-transformed centroid size summarizes the association between shape and size (regression score 1) and accounts for 30.1% of the predicted variance (males = 10.5%; females = 14.3%; $p < 0.0001$). Figure 7a (males) and b (females) shows the distribution of groups along the allometric scaling relationship, which replicates the pattern of group distribution seen along PC1, i.e., the larger species *P. ursinus*, *P. anubis* and *P. cynocephalus* north and south are clustered on one side of the distribution, the medium-sized *P. papio* and *P. hamadryas* are intermediate, and the smaller *P. kindae* falls together with *P. cynocephalus* DRC on the opposite side.

3.4. Canonical variates and discriminant function analyses before and after size correction

The result of the CVA and DFA on Procrustes shape coordinates and "size-corrected" shape coordinates between groups before and after correcting for size are given in Figure 8a,b and Tables 4—7 respectively. Male DFA before size correction was unable to differentiate between Gorongosa/*P. ursinus griseipes*, *P. ursinus*/*P. ursinus griseipes*, *P. cynocephalus* south/*P. ursinus griseipes*, *P. cynocephalus*
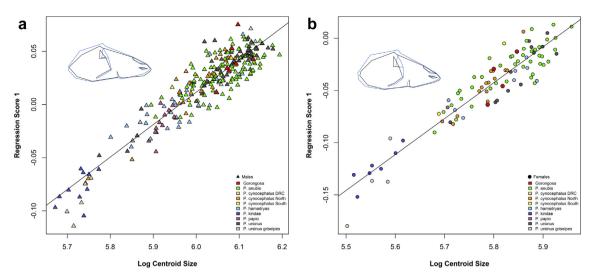
Figure 7. (a−b). Regression score 1 (30.1% of variation explained) and log centroid size plot. Wireframes represent extremes of size-correlated shape variation: black wireframes are associated with large cranial size. Blue wireframes are associated with small cranial size. The projection of the face relative to the braincase increases with larger cranial size. The relative height of the skull decreases with larger cranial size. a) Males (10.5% of variation explained). b) Females (14.3% of variation explained).
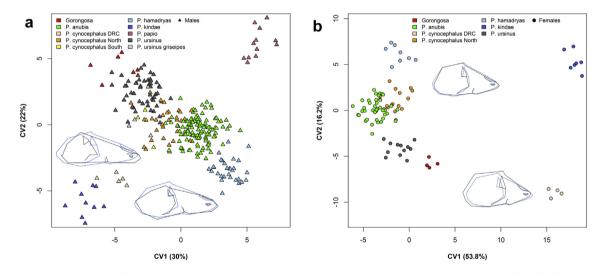

Figure 8. a) Canonical variates (CVs) plot for males (variance: CV1 = 30%; CV2 = 22%). Gorongosa National Park baboons are at one extreme of the distribution, overlapping with *P. ursinus*. The *P. kindae* and *P. cynocephalus* DRC groups cluster together. Beside *P. papio* and *P. kindae/P. cynocephalus* DRC, all other groups are distributed along a continuum. CV1 summarizes variation associated with a decrease of the relative height of the skull towards the positive end of the distribution. CV2 summarizes shape variation associated with an increase in the projection of the face relative to the braincase towards the positive end of the distribution. b) Canonical variates plot for females (variance: CV1 = 53.8%; CV2 = 16.2%). CV1 separates *P. kindae/P. cynocephalus* DRC from all other groups. GNP baboons are at one extreme of the distribution along CV2. Wireframes represent extremes of shape variation. Black wireframes: positive end of the distribution. Blue wireframes: negative end of the distribution.

south/*P. ursinus*, *P. cynocephalus* south/*P. cynocephalus* north, and *P. kindae/P. cynocephalus* DRC (Table 4). Female DFA before size correction was unable to differentiate between Gorongosa/*P. ursinus*, *P. ursinus/P. hamadryas*, *P. hamadryas/P. cynocephalus* north, and *P. kindae/P. cynocephalus* DRC (Table 5). Male DFA on "size-corrected" shape maintained similar results but was also unable to differentiate the *P. cynocephalus* north/*P. ursinus griseipes* pair (Table 6). Female DFA on "size-corrected" shape also was unable to differentiate the Gorongosa/*P. ursinus* and *P. kindae/P. cynocephalus* DRC pairs, and also *P. hamadryas/P. cynocephalus* north and *P. hamadryas/P. anubis* (Table 7). From these pairs of undifferentiated groups, we were interested in confirming *P. cynocephalus* south/*P. u. griseipes*. Because of small group sizes, DFA cross-validation shows difficulties in allocating *P. cynocephalus* south/*P. u. griseipes* before and after correcting for size (Table 8; the reliability of the discrimination is assessed by leave-one-out cross-validation).

Figure 8a and b shows the male and female CVA plots of "size-corrected" shape coordinates (similar results were obtained before size correction). For male CVA (Fig. 8a; CV1 = 30%; CV2 = 22%), the GNP baboons are at one end of the distribution, overlapping with *P. ursinus*. The *P. kindae* and *P. cynocephalus* DRC groups cluster together. Beside *P. papio* and *P. kindae/P. cynocephalus* DRC, all of the other groups are distributed along a continuum. *Papio anubis* is intermediate between *P. hamadryas* and *P. cynocephalus*, whereas *P. ursinus* encompasses all *P. ursinus griseipes* and most of *P. cynocephalus* south. A few *P. cynocephalus* north and south individuals are actually closer to the *P. kindae/P. cynocephalus* DRC cluster. Canonical variate (CV) 1 summarizes variation associated with a decrease of the relative height of the skull (Fig. 8a; CV1, positive end of the distribution), and CV2 summarizes variation associated with an increase in the projection of the face (facial length and molar row position) relative to the braincase (Fig. 8a;

Table 4
Procrustes distances among groups (males) before correcting for size (*p* values from 1000 permutation test rounds).[a]

Males								
	Gorongosa	P. anubis	P. c. DRC	P. c. north	P. c. south	P. hamadryas	P. kindae	P. papio	P. ursinus
P. anubis	**0.0578 (<0.001)**								
P. cynocephalus DRC	**0.1518 (<0.001)**	**0.1304 (<0.001)**							
P. cynocephalus north	**0.0582 (<0.001)**	**0.2697 (<0.001)**	**0.1146 (<0.001)**						
P. cynocephalus south	**0.0489 (0.005)**	**0.0413 (0.007)**	0.12560.006	0.0320 (0.298)					
P. hamadryas	**0.0817 (<0.001)**	**0.0438 (<0.001)**	**0.0991 (<0.001)**	**0.0392 (<0.001)**	**0.0568 (<0.001)**				
P. kindae	**0.1379 (<0.001)**	**0.1183 (<0.001)**	0.0031 0.1860	**0.1008 (<0.001)**	**0.1122 (<0.001)**	**0.0887 (<0.001)**			
P. papio	**0.0879 (<0.001)**	**0.0569 (<0.001)**	**0.0927 (<0.001)**	**0.0501 (<0.001)**	**0.0665 (0.001)**	**0.0412 (<0.001)**	**0.0846 (<0.001)**		
P. ursinus	**0.0407 (<0.001)**	**0.0390 (<0.001)**	**0.1412 (<0.001)**	**0.0362 (<0.001)**	0.0313 (0.165)	**0.0651 (<0.001)**	**0.1272 (<0.001)**	**0.0740 (<0.001)**	
P. ursinus griseipes	0.04378 (0.1390)	**0.04370.003**	**0.1472 (0.007)**	**0.0438 (0.037)**	0.0401 (0.275)	**0.0711 (<0.001)**	**0.1325 (0.001)**	**0.0814 (0.001)**	0.0242 (0.695)

[a] Significant results at <0.05 are shown in bold.

Table 5
Procrustes distances among groups (females) before correcting for size (*p* values from 1000 permutation test rounds).[a]

Females (P. papio and P. cynocephalus south are excluded due to small sample size)					
	Gorongosa	P. anubis	P. c. DRC	P. c. north	P. hamadryas	P. kindae
P. anubis	**0.0466 (0.002)**					
P. cynocephalus DRC	**0.1175 (0.004)**	**0.1234 (<0.001)**				
P. cynocephalus north	**0.0448 (0.025)**	**0.0249 (0.004)**	**0.1076 (<0.001)**			
P. hamadryas	**0.0475 (0.038)**	**0.0277 (0.042)**	**0.109 (0.002)**	0.0278 (0.199)		
P. kindae	**0.1035 (0.002)**	**0.1104 (<0.001)**	0.0334 (0.423)	**0.0940 (<0.001)**	**0.0962 (<0.001)**	
P. ursinus	0.0431 (0.078)	**0.0276 (0.004)**	**0.1252 (<0.001)**	**0.0317 (0.03)**	0.0348 (0.055)	**0.1127 (<0.001)**

[a] Significant results at <0.05 are shown in bold.

Table 6
Procrustes distances among groups (males) after correcting for size (*p* values from 1000 permutation test rounds).[a]

Males								
	Gorongosa	P. anubis	P. c. DRC	P. c. north	P. c. south	P. hamadryas	P. kindae	P. papio	P. ursinus
P. anubis	**0.0568 (<0.001)**								
P. cynocephalus DRC	**0.0850 (<0.001)**	**0.0582 (<0.001)**							
P. cynocephalus north	**0.0517 (<0.001)**	**0.0217 (<0.001)**	**0.0582 (<0.001)**						
P. cynocephalus south	**0.0452 (0.070)**	**0.0413 (0.003)**	**0.0688 (0.021)**	0.0314 (0.135)					
P. hamadryas	**0.0694 (<0.001)**	**0.0286 (<0.001)**	**0.0542 (<0.001)**	**0.0357 (<0.001)**	**0.0520 (<0.001)**				
P. kindae	**0.0731 (<0.001)**	**0.0490 (<0.001)**	0.0320 (0.145)	**0.0446 (<0.001)**	**0.0564 (0.004)**	**0.0483 (<0.001)**			
P. papio	**0.0667 (<0.001)**	**0.0301 (<0.001)**	**0.0622 (<0.001)**	**0.0401 (<0.001)**	**0.0557 (<0.001)**	**0.0385 (<0.001)**	**0.0597 (<0.001)**		
P. ursinus	**0.0402 (<0.001)**	**0.0387 (<0.001)**	**0.0725 (<0.001)**	**0.0290 (<0.001)**	0.0283 (0.172)	**0.0527 (<0.001)**	**0.0596 (<0.001)**	**0.0592 (<0.001)**	
P. ursinus griseipes	0.0434 (0.092)	**0.0422 (0.008)**	**0.0730 (0.023)**	0.0336 (0.059)	0.034 (0.459)	**0.0553 (0.001)**	**0.0586 (0.001)**	**0.0591 (<0.001)**	0.0232 (0.640)

[a] Significant results at<0.05 are shown in bold.

CV2, positive end of the distribution). For female CVA (Fig. 8b), CV1 (53.8%) separates *P. kindae* and *P. cynocephalus* DRC from the rest. The separation is greater than the separation observed in the male CVA. This is most likely due to the absence of *P. papio* in the female CVA (Fig. 8b). Along CV2 (16.2%), the GNP baboons are grouped closer to *P. ursinus*. Interestingly, if we contrast the proximity of all groups to the *P. kindae/P. cynocephalus* DRC cluster along CV1 (53.8%), the GNP baboon group is the only one that deviates from the cluster formed by *P. hamadryas, P. cynocephalus* north, *P. anubis,* and *P. ursinus*. This could suggest some sort of low degree of proximity between the female GNP baboons and the *P. kindae/P. cynocephalus* DRC cluster. Canonical variate 1 summarizes variation associated with an increase of the relative height of the skull and a decrease in the relative projection of the face (Fig. 8b; CV1, positive end of the distribution. Canonical variate 2 summarizes variation associated with a subtle increase in the projection of the face relative to the braincase (Fig. 8b; CV2, positive end of the distribution).

3.5. PCA of averaged groups and agglomerative-hierarchical cluster analysis

Figure 9a and b shows the results from the PCA for group mean configurations. For males (Fig. 9a), PC1 summarizes 49.9% of the explained variance and represents shape variation related to klinorhynchy. Principal component 2 explains 21.5% and represents shape variation in the relative breadth of the middle face observed in the malar surface and the orbital process of the zygomatic bone (Fig. 9a). The distribution of the mean configurations shows that Gorongosa baboons are closer to *P. ursinus, P. ursinus griseipes,* and *P. cynocephalus* south, while *P. cynocephalus* north, *P. anubis,*

Table 7
Procrustes distances among groups (females) after correcting for size (*p* values from 1000 permutation test rounds).[a]

Females (*P. papio* and *P. cynocephalus* south are excluded due to small sample size)						
	Gorongosa	*P. anubis*	*P. c.* DRC	*P. c.* north	*P. hamadryas*	*P. kindae*
P. anubis	**0.0454 (<0.001)**					
P. cynocephalus DRC	**0.0637 (0.033)**	**0.0600 (<0.001)**				
P. cynocephalus north	**0.0439 (0.007)**	**0.0180 (0.022)**	**0.0584 (<0.001)**			
P. hamadryas	**0.0471 (0.009)**	0.0234 (0.055)	**0.0585 (0.004)**	0.0289 (0.06)		
P. kindae	**0.05773 (<0.001)**	**0.0559 (<0.001)**	0.0326 (0.401)	**0.0523 (<0.001)**	**0.0555 (0.001)**	
P. ursinus	0.0426 (0.008)	**0.0282 (<0.001)**	**0.0659 (<0.001)**	**0.0289 (0.015)**	**0.0315 (0.046)**	**0.0636 (<0.001)**

[a] Significant results at <0.05 are shown in bold.

Table 8
Classification and misclassification DFA cross-validations for males *P. u. griseipes*/*P. cynocephalus* south, before and after size correction (reliability of the discrimination is assessed by leave-one-out cross-validation).

	Allocated to (before size correction)		Total
	P. u. griseipes	*P. c.* south	
P. u. griseipes	2	2	4
P. c. south	4	0	4
	(after size correction)		
P. u. griseipes	2	2	4
P. c. south	4	0	4

P. hamadryas, and *P. papio* form a more loose-fitting cluster. *Papio kindae* falls closer to *P. cynocephalus* DRC, and both are apart from other group means. For females (Fig. 9b), PC1 summarizes 48.1% of the explained variance and PC2 explains 21.4%. Principal component 1 represents shape variation related to the elongation of the face; PC2 represents shape variation related to the breadth of the middle face (Fig. 9b). The distribution of the mean configurations shows that Gorongosa baboons fall between *P. ursinus* and *P. cynocephalus* south (Fig. 9b). *Papio cynocephalus* north, *P. anubis*, *P. hamadryas*, and *P. ursinus* form a loose-fitting cluster. *Papio kindae* falls closer to *P. cynocephalus* DRC, and both are apart from other group means. The PC3 and PC4 for male and female between-groups PCA are shown in Figure 10.

Figures 11 and 12 show the phenograms from cluster analyses to situate Gorongosa baboons within the craniofacial variability of the genus *Papio*. For males, the first UPGMA tree (Fig. 11a) shows a dichotomy between the southern and northern baboons. The northern branch clusters *P. anubis* and *P. cynocephalus* north, *P. hamadryas*, and then *P. papio*. The southern branch clusters *P. ursinus* and *P. ursinus griseipes*, and then *P. cynocephalus* south. Gorongosa falls within this southern branch, similar to the other members of this clade: *P. cynocephalus* south, *P. ursinus*, and *P. ursinus griseipes*. The smaller baboons, *P. kindae* and *P. cynocephalus* DRC, are grouped together in a branch outside of the northern and southern variation. When Ward's method was applied (Fig. 11b), larger distances between the northern and southern branches emerge and, possibly as a consequence, *P. kindae* and *P. cynocephalus* DRC cluster with the northern branch. For females, the first UPGMA tree (Fig. 12a) does not reproduce the dichotomy between the southern and northern baboons. However, when Ward's method is applied, the dichotomy reappears, and locates *P. cynocephalus* south outside the north and south branches (Fig. 12b).

Figures 11c−d and 12c−d show the comparative trees excluding PC3. For females, this procedure worked well because we observe an equidistant separation between Gorongosa and the rest of the female averages (Fig. 10b; PC3 = 14.4%). However, the separation is not equidistant for male group means (PC3 = 9.6%; Fig. 10a). Thus, we place more confidence in the female phenograms after performing this correction (Fig. 12c−d). The results for males and females mostly replicated the general topology of the previous trees,
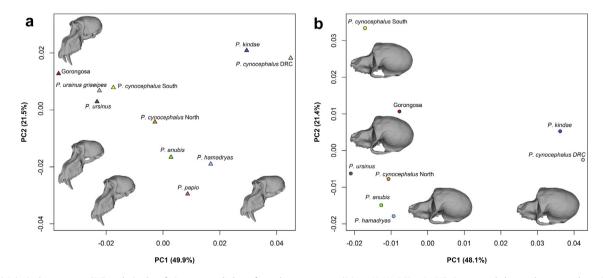

Figure 9. a) Principal component (PC) analysis plot of 'size corrected' shape for male group means (PC1 = 49.9%; PC2 = 21.5%). Gorongosa baboons cluster together with *P. ursinus*, *P. ursinus griseipes* and P. *cynocephalus* south, while *P. cynocephalus* north, *P. anubis*, *P. hamadryas* and *P. papio* form a different cluster. *P. kindae* falls closer to *P. cynocephalus* DRC and both are apart from other group means. PC1 represents shape changes related to klinorhynchy. PC2 represents shape changes related to the breadth of the middle face. b) PCA plot of 'size corrected' shape for female group means (PC1 = 48.1%; PC2 = 21.4%). Gorongosa baboons cluster between *P. ursinus* and P. *cynocephalus* south. PC1 represents shape changes related to the elongation of the face. PC2 represents shape changes related to the breadth of the middle face.
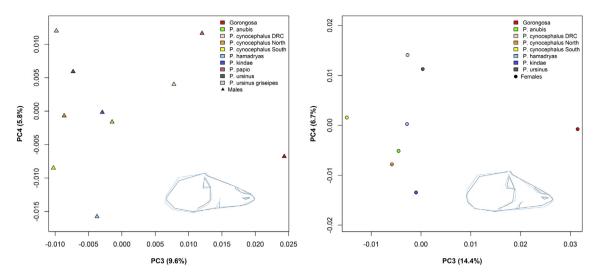
Figure 10. Principal components (PC) 3 and 4 for male (a) and female (b) between-groups PCA. PC3 summarizes most of the differences between the Gorongosa consensus and all other mean configurations in males and females. Wireframes represent extremes of shape variation along PC3. Black wireframes: positive end of the distribution. Blue wireframes: negative end of the distribution.

with a few exceptions. For the male phenograms (Fig. 11c—d), Gorongosa clusters closer to *P. ursinus griseipes* and *P. ursinus* than *P. cynocephalus* south, but the relative position of *P. papio* and *P. hamadryas* is inverted in the northern branch. For the female UPGMA tree (Fig. 12c), *P. cynocephalus* south and Gorongosa cluster together; however, *P. ursinus* clusters with the northern branch. On the other hand, the female phenogram tree resulting from Ward's method (Fig. 12d) supports the association of *P. cynocephalus* south and Gorongosa, and places *P. ursinus* in the southern branch.

3.6. Genetic and phenetic Mantel correlograms

Tables 9—12 show the results of the Mantel tests. Only the "size-corrected" shape coordinates yielded a statistically significant "overall" Mantel correlation (rM = 0.121; p = 0.001; Table 9); also for males (rM = 0.161; p = 0.001; Table 10) and females (rM = 0.152; p = 0.021; Table 11). The genetic correlograms produced a statistically significant "overall" Mantel correlation (rM = 0.411; p value = 0.001; Table 12).

Figure 13 shows the "size-corrected" shape correlograms (Fig. 13a—c) and the CYT-B gene Mantel correlogram (Fig. 13d). The genetic and shape correlogram plots display a shared pattern of genetic similarity decay with respect to geographic distance. The CYT-B gene Mantel correlogram shows a pronouncedly steep pattern, starting with moderate positive correlation in the first distance class (class 1: 0—1109 km; rM = 0.338; p = 0.001; Table 12) and declining towards significantly negative correlations. The "size-corrected" shape correlogram (combined sexes) shows low positive correlation in the first distance class (class 1: 0—1153 km; rM = 0.132; p = 0.001; Table 9) and a small decrease towards negative correlations, with a flat pattern from 2306 km (classes 3—6) and no statistical significance after 3459 km (classes 4—6). In short, both the genetics and the morphology correlate positively at shorter geographic distances, but the correlation decreases as geographic distance increases, as expected under an isolation-by-distance model.

4. Discussion

In this work, we set out to provide the first morphological assessment of the baboons in GNP, a population located close to a

predicted contact area between *P. cynocephalus* and *P. ursinus*. We describe their external phenotype based on fourteen traits and compared these features to those observed in both *P. ursinus griseipes* and *P. cynocephalus*. Then, we implemented geometric morphometric techniques to place the GNP baboons within *Papio* diversity. Our results show their morphology is a combination of features, or a mosaic between *P. ursinus griseipes* and *P. cynocephalus* south.

As described by previous research, baboon craniofacial shape variation is highly related to size (Leigh and Cheverud, 1991; O'Higgins and Collard, 2002; Singleton, 2002; Frost et al., 2003; Leigh, 2006; Singleton et al., 2017) and geographic origin (Frost et al., 2003; Dunn et al., 2013). In our study, we found that allometry explains more than 30% of shape variation, which is close to the 35% described by Frost et al. (2003). After removing the effects of size, craniofacial shape allowed us to place the baboons from Gorongosa in close relation to *P. ursinus griseipes* and *P. cynocephalus* south, which is expected in the light of their geographic location. The "size-corrected" shape PCA averaged by groups and agglomerative-hierarchical cluster analysis reproduced the well-established subdivision of the genus *Papio* in the north and south clades (Jolly, 2003; Frost et al., 2003; Zinner et al., 2009). Within the northern clade, cluster analysis was concordant with the topology of mtDNA-based phylogenetic trees showing eastern olive baboons and northern yellow baboons as forming a single clade, with hamadryas being closer to this clade than Guinea baboons (see McGoogan et al., 2007). The Kinda clade is less stable and is closely related to *P. cynocephalus* DRC specimens, which indicates that the latter are Kinda baboons labeled as *P. cynocephalus* before they were recognized as an independent taxon. MtDNA molecular data have placed Kinda baboons within the southern branch. However, our results suggest that, at least with respect to "size-corrected" shape, the Kinda tends to separate from the rest as a third independent clade. This finding is in agreement with results from Singleton et al. (2017) showing that the Kinda baboon differs from other species in its size, shape, and size-independent shape dimorphism patterns. The fact that Kinda falls within the northern clade when applying Ward's clustering method could be indicative of some sort of affinity with the northern clade. More complex demographic scenarios involving admixture between members of the northern and southern clade
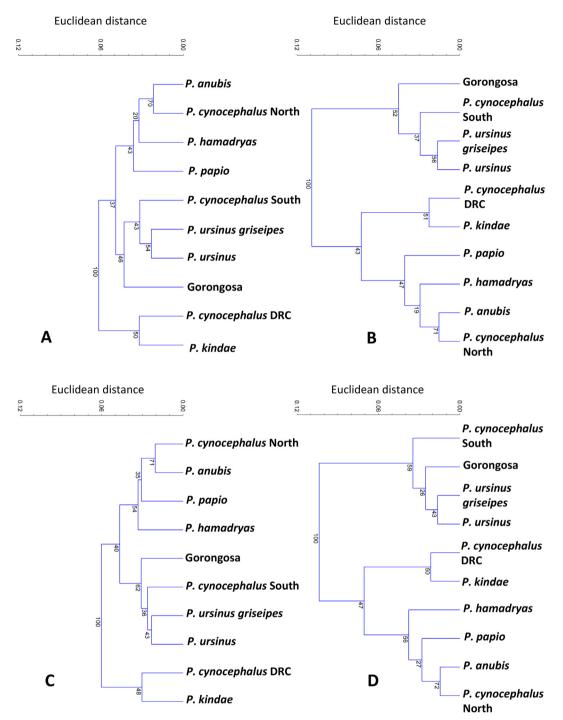
Figure 11. Agglomerative clustering trees for males. UPGMA (A) and Ward's method (B) using all principal components (PC) of group means. UPGMA (C) and Ward's method (D) excluding one component (PC3: 9.6% explained variance) summarizing most differences between Gorongosa and all other groups in order to control for scanning error.

in generating the morphological peculiarity of the Kinda baboons might also be possible (see Rogers et al., 2019).

One unique aspect of our analysis as compared to previous morphometric studies (see Frost et al., 2003; Dunn et al., 2013; Singleton et al., 2017) was that we took into account the mtDNA paraphyly of *P. cynocephalus* and treated the north and south yellow baboons separately. Zinner et al. (2009) showed that north and south yellow baboons fall into different mtDNA clades. Furthermore, Zinner et al. (2015) delineated a division between north and south yellow baboon mtDNA clades along the Ugalla-Malagarasi

River and Ruaha-Rufiji River in central Tanzania. Our results based on this approach fit the published molecular data well. More generally, they match up with the idea of a differentiation between southern and northern yellow baboons. Moreover, the clustering of male GNP baboons with male chacma (Fig. 11c—d), and female GNP baboons with female southern yellow (Fig. 12c—d) allow us to put forward, at least from skull morphology, an affinity of the GNP baboons with both the southern yellow and chacma baboons. In addition, DFA was unable to differentiate between grayfooted chacma males and southern yellow males, which all together,
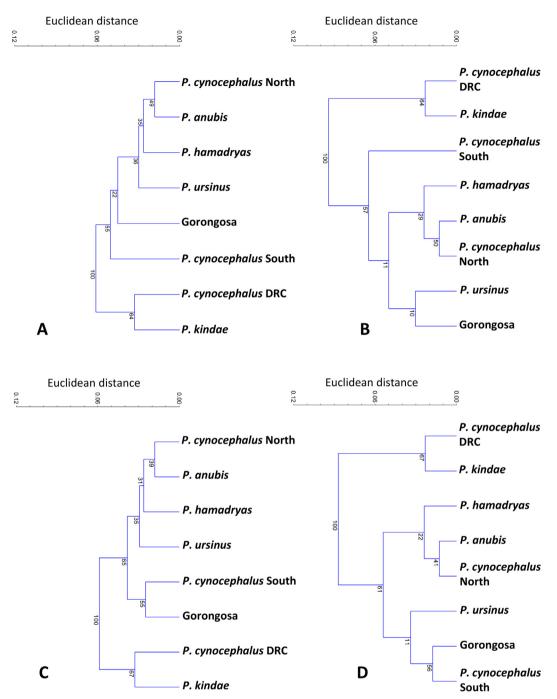
Figure 12. Agglomerative clustering trees for females. UPGMA (A) and Ward's method (B) using all principal components (PC) of group means. UPGMA (C) and Ward's method (D) excluding one component (PC3: 14.4% explained variance) summarizing most differences between Gorongosa and all other groups in order to control for scanning error.

Table 9
Mantel correlogram results for "size-corrected" shape and geographic distances with 999 permutations (combined sexes).

Overall Mantel statistic r (rM) = 0.121; significance: 0.001				
Class	Distance range (km)	rM	p	Bonferroni corrected p
1	0–1153	0.132	0.001	0.001
2	1153–2306	−0.032	0.02	0.04
3	2306–3459	−0.058	0.002	0.006
4	3459–4612	−0.051	0.013	0.052
5	4612–5765	−0.027	0.121	0.605
6	5765–6918	−0.030	0.075	0.450

suggest that the GNP baboon phenotype fits within a geographic clinal pattern of replacing allotaxa. In conclusion, our results, indicating that the GNP baboons constitute a mosaic form between the yellow and the chacma, support the hypothesis of either past and/or ongoing hybridization between the grayfooted chacma and southern yellow baboons in GNP or an isolation-by-distance scenario with GNP baboons geographically and morphologically intermediate between the chacma and southern yellow baboons. The two scenarios are not mutually exclusive, as gene flow between neighboring groups could have also happened after the initial dispersal. The affinity of the female GNP baboons and female

Table 10
Mantel correlogram results for male "size-corrected" shape and geographic distances with 999 permutations.

Overall Mantel statistic r (rM) = 0.161; significance: 0.001				
Class	Distance range (km)	rM	p	Bonferroni corrected p
1	0—1141	0.163	0.001	0.001
2	1141—2282	−0.000	0.460	0.920
3	2282—3423	−0.099	0.001	0.003
4	3423—4564	−0.071	0.006	0.024
5	4564—5706	−0.030	0.120	0.600
6	5706—6848	−0.045	0.059	0.354

Table 11
Mantel correlogram results for female "size-corrected" shape and geographic distances with 999 permutations.

Overall Mantel statistic r (rM) = 0.152; significance: 0.021				
Class	Distance range (km)	rM	p	Bonferroni corrected p
1	0—1125	0.194	0.001	0.001
2	1125—2251	−0.141	0.002	0.004
3	2251—3377	−0.025	0.249	0.747
4	3377—4502	−0.013	0.338	1.352
5	4502—5628	−0.045	0.129	0.645
6	5628—6755	−0.039	0.194	1.164

Table 12
Mantel correlogram results for genetic (CYT-B gene) and geographic distances with 999 permutations.

Overall Mantel statistic r (rM) = 0.411; significance: 0.001				
Class	Distance range (km)	rM	p	Bonferroni corrected p
1	0—1109	0.338	0.001	0.001
2	1109—2218	0.076	0.001	0.002
3	2218—3327	−0.127	0.001	0.003
4	3327—4436	−0.188	0.001	0.004
5	4436—5545	−0.194	0.001	0.005
6	5545—6655	−0.097	0.001	0.006

southern yellow, and the affinity of the male GNP baboons and male chacma, could be an indication of recent hybridization.

As Jolly (1993) pointed out, some confusion existed in the past as to whether baboons from northern Mozambique, Malawi, and northwestern Zambia belong to *P. ursinus* or *P. cynocephalus*. Earlier authors interpreted this as evidence of admixture between the chacma and the yellow (Napier, 1981) or as evidence of a chacma/yellow cline (Freedman, 1963; Booth and Freedman, 1970). Currently, there is agreement that the Luangwa baboons from eastern Zambia and Malawi are considered to be *P. cynocephalus jubilaeus* (Burrell, 2009; Zinner et al., 2015). Some authors have described finding *P. cynocephalus strepitus* in Malawi, and north-central Mozambique (Hill, 1970), including the Catapu Forest Reserve (Zinner et al., 2015), located in the southern margin of the Zambezi River and 120 km north to GNP. In fact, baboons from Catapu exhibit yellow features (yellow fur, white ventral hair, circum-orbital pink skin, silvery fringe on hands and feet). However, the Mozambican Lower Zambezi is a wide river, which baboons are unlikely to swim across. On the other hand, we could not discard a scenario where ancient changes in the drainage system of the Lower Zambezi River (Cotterill, 2003, 2006; McCartney and Owen, 2007; Rocha, 2014) led to secondary contact between yellow and grayfooted chacma baboons. If this were the case, GNP would be an area of hybridization.

Several phenotypic and mtDNA features link the GNP baboons to both the *P. cynocephalus* south and *P. ursinus griseipes*. This phenostructure pattern would be expected under an ongoing process of nuclear swamping and/or past admixture, rather than lineage sorting. The genetic mtDNA data available for *Papio* include two samples collected from GNP (Zinner et al., 2009). The GNP baboon mtDNA falls within haplogroup B, which is shared by the southern yellow and northern chacma baboons (as mentioned, the distribution of the northern chacma subclade most likely coincides with the subspecies *P. u. griseipes*). South yellow and grayfooted chacma mtDNA form their own subclades within haplogroup B, while the mtDNA data from Gorongosa fall near the grayfooted chacma in the northern subclade of haplogroup B (preliminary data from an ongoing study of a larger set of samples agree with these observations). More genetic data, also analyzing the variation at the nuclear level, are necessary to fully investigate the relationships between the GNP, southern yellow, and northern chacma baboons, and to explore the underlying evolutionary dynamics (like primary or secondary hybridization).

Interestingly, Keller et al. (2010) found the same mtDNA haplotype from Gorongosa in Moremi National Park (Okavango Delta, Botswana), more than 1200 km away from Gorongosa (haplotype NC7; Keller et al., 2010). Keller et al. (2010) also found this haplotype in Rhodes Inyanga National Park (Zimbabwe) and Alldays (Republic of South Africa). The latter is located 670 km southwest of Gorongosa and 740 km southeast of Moremi, drawing a triangular area of 238,646 km². Zinner et al. (2009) found mtDNA haplotypes belonging to the same clade more than 1100 km apart in Namibia and South Africa. These findings are compatible with ancient shared haplotypes and/or a significant amount of past, recent, or ongoing gene flow across the grayfooted chacma baboon populations (see Sithaldeen et al., 2009, 2015) and are consistent with our Mantel correlation results. This level of gene flow may not be unexpected for baboons, given their behavioral flexibility and ability to use different habitats. Habitat modeling in West Africa by Vale et al. (2015) showed a high degree of association between baboons' occurrence and water and the authors suggested that river valleys could represent adequate ecological corridors for baboons. In the more dry landscape of southern Africa, river valleys may have an even more important role as corridors. Gorongosa and Moremi localities are connected through the Zambezi River Valley, which is thought to have a major impact on the biogeographic structure and evolution of southern African mammal species (Cotterill, 2003; Pedersen et al., 2018). Thus, one possible explanation underlying the shared haplotypes between Moremi and Gorongosa, is that the Zambezi River Valley functions as a corridor and allows functional connectivity between distant populations of grayfooted baboons.

The results from the Mantel correlations show a positive relationship for genetic diversity at geographic distances within 1100 km. This relationship decreases as geographic distance increases, as would be expected under an isolation-by-distance model. This result agrees with previous research suggesting isolation-by-distance using a Mantel correlation between genetic and geographic distance for different baboon species (Ferreira da Silva et al., 2014; Kopp et al., 2014, 2015). In our study, only after removing the effects of size does morphology correlate with the above-mentioned genetic pattern. The lack of correlation when looking at craniofacial morphology at longer distances might be due to drift or local pressures, which make it deviate from simple linearity. It is likely that at longer distances, many of the comparisons end up being across different ecological zones. The match between genetic and morphological correlation to geographic distance validates the use of the "size-corrected" craniofacial shape in our comparative morphometric analysis and confirms that, after the effects of size are removed, craniofacial complexity still retains population history signals (Cardini and Elton, 2008).

Finally, these results provide new evidence and a novel framework to interpret the evolutionary processes influencing the
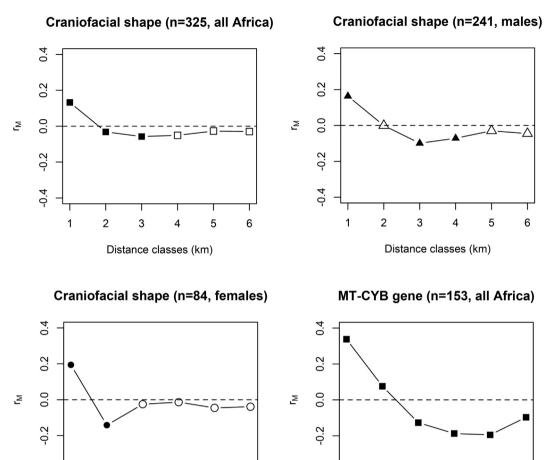
Craniofacial shape (n=325, all Africa)

Craniofacial shape (n=241, males)

Craniofacial shape (n=84, females)

MT-CYB gene (n=153, all Africa)

Figure 13. a) Mantel correlogram for 'size-corrected' craniofacial shape distance (combined sexes). The 'size-corrected' shape correlogram shows low positive correlation in the first distance class (class 1: 0−1153 km; rM = 0.132; p = 0.001) and a small decrease towards negative correlations, with a flat pattern from 2306 km (classes 3−6) and no statistical significance after 3459 km (classes 4−6; see Table 9). b) Males show a similar pattern with low positive correlation in the first distance class (class 1: 0−1141 km; rM = 0.163; p = 0.001) and a small decrease towards negative correlations, with a flat pattern from 2282 km (classes 3−6) and no statistical significance after 4564 km (classes 5 and 6; see Table 10). c) Females also show low positive correlation in the first distance class (class 1: 0−1125 km; rM = 0.194; p = 0.001), but low negative correlation in class 2 (1125−2251 km; rM = −0.141; p = 0.004) and a flat pattern with no statistical significance after 2251 km (classes 3−6; see Table 11). d) Mantel correlogram for genetic distance shows a pronounced steep pattern, starting with moderate positive correlation in the first distance class (class 1: 0−1109 km; rM = 0.338; p = 0.001) that decreases towards significant negative correlations (see Table 12).

diversity, distribution, and structure of *Papio* species. More broadly, papionin species have long been considered a useful model to understand processes occurring in early human evolution (Jolly, 2001). The data provided here might be useful in the interpretation of hominin fossils separated by distances similar to those of *Papio* populations (in some cases, >1000 km). For example, middle Pleistocene hominins from sites such as Bodo (Ethiopia), Kabwe (Zambia), and Elandsfontein (South Africa), may be considered representative of different species or populations of a species, depending on the framework for comparison (Rightmire, 2013). The baboon data provide a useful empirical framework for considering variation and possible gene flow across widely separated early hominin populations (or species).

Author contributions

S.C. and R.B. conceived and co-direct the PPP project. F.I.M., C.C. and M.F.d.S. conceived the morphometric and genetics study. F.I.M.

analyzed the data and wrote the manuscript. C.C., M.F.d.S., R.B. and S.C. contributed to manuscript writing. V.A., Z.A., W.A., M.B., D.B., D.R.B., E.C., J.H., T.L., H.M., J.M., L.M.P., M.P., M.S. and F.T. contributed to fieldwork and edited the manuscript. All authors read and approved the final version of the manuscript.

Supplementary Online Material

Supplementary online material related to this article can be found at https://doi.org/10.1016/j.jhevol.2019.01.007.

References

Altmann, J., Altmann, S., Hausfater, G., 1981. Physical maturation and age estimates of yellow baboons, *Papio cynocephalus*, in Amboseli National Park, Kenya. American Journal of Primatology 1, 1389–1399.

Alberts, S., Altmann, J., 2001. Immigration and hybridization patterns of yellow and anubis baboons in and around Amboseli, Kenya. American Journal of Primatology 53, 139–154.

Barrett, L., Henzi, S.P., 2008. Baboons. Current Biology 18, R404–R406.

Bookstein, F.L., 1991. Morphometric Tools for Landmark Data: Geometry and Biology. Cambridge University Press, Cambridge.

Booth, S., Freedman, L., 1970. Multivariate discriminant analysis applied to cranial features of *P. ursinus* and *P. cynocephalus*. Folia Primatologica 12, 276–289.

Borcard, D., Legendre, P., 2012. Is the mantel correlogram powerful enough to be useful in ecological analysis? A simulation study. Ecology 93, 1473–1481.

Burrell, A., 2009. Phylogenetics and population genetics of Central African baboons. PhD thesis. New York University, Department of Anthropology.

Cardini, A., Elton, S., 2008. Does the skull carry a phylogenetic signal? Evolution and modularity in the guenons. Biological Journal of the Linnean Society 93, 813–834.

Cardini, A., Jansson, A.-U., Elton, S., 2007. A geometric morphometric approach to the study of ecogeographical and clinal variation in vervet monkeys. Journal of Biogeography 34, 1663–1678.

Chiou, K.L., 2018. http://kennychiou.com/dissertation/ (accessed 28.02.18).

Copes, L.E., Lucas, L.M., Thostenson, J.O., Hoekstra, H.E., Boyer, D.M., 2016. A collection of non-human primate computed tomography scans housed in MorphoSource, a repository for 3D data. Science Data 3, 160001.

Collard, M., O'Higgins, P., 2001. Ontogeny and homoplasy in the papionin monkey face. Evolution and Development 3, 322–331.

Cotterill, F.P.D., 2003. Geomorphological influences on vicariant evolution in some African mammals in the Zambezi Basin: some lessons for conservation. In: Plowman, A. (Ed.), Ecology and Conservation of Mini-antelope: Proceedings of an International Symposium on Duiker and Dwarf Antelope in Africa. Filander Verlag, Fürth/Germany, pp. 11–58.

Cotterill, F.P.D., 2006. The Evolutionary History and Taxonomy of the Kobus Leche Species Complex of South-Central Africa in the Context of Palaeo-drainage Dynamics. Stellenbosch University, Stellenbosch.

Cracraft, J., 1983. Species concepts and speciation analysis. In: Johnston, R.F. (Ed.), Current Ornithology. Plenum Press, New York, pp. 159–187.

Diniz-Filho, J.A.F., Soares, T.N., Lima, J.S., Dobrovolski, R., Landeiro, V.L., de Campos Telles, M.P., Rangel, T.F., Bini, L.M., 2013. Mantel test in population genetics. Genetics and Molecular Biology 36, 475–485.

Dobzhansky, T., 1937. Genetics and the Origin of Species. Columbia University Press, New York.

Drake, A.G., Klingenberg, C.P., 2008. The pace of morphological change: historical transformation of skull shape in St Bernard dogs. Proceedings of the Royal Society B 275, 71–76.

Dray, S., Dufour, A.B., 2007. The ade4 package: implementing the duality diagram for ecologists. Journal of Statistical Software 22, 1–20.

Dunbar, R.I.M., 1990. Environmental determinants of intraspecific variation in body weight in baboons (*Papio* spp.). Journal of Zoology 220, 157–169.

Dunn, J., Cardini, A., Elton, S., 2013. Biogeographic variation in the baboon: dissecting the cline. Journal of Anatomy 223, 337–352.

Ferreira da Silva, M.J., Godinho, R., Casanova, C., Minhós, T., Sá, R., Bruford, M.W., 2014. Assessing the impact of hunting pressure on population structure of Guinea baboons (*Papio papio*) in Guinea-Bissau. Conservation Genetics 15, 1339–1355.

Fischer, J., Kopp, G.H., Dal Pesco, F., Goffe, A., Hammerschmidt, K., Kalbitzer, U., Klapproth, M., Maciej, P., Ndao, I., Patzelt, A., Zinner, D., 2017. Charting the neglected West: The social system of Guinea baboons. American Journal of Physical Anthropology 162, 15–31.

Freedman, L., 1963. A biometric study of *Papio cynocephalus* skulls from northern Rhodesia and Nyasaland. Journal of Mammalogy 44, 24–43.

Frost, S.R., Marcus, L.F., Bookstein, F.L., Reddy, D.P., Delson, E., 2003. Cranial allometry, phylogeography, and systematics of large-bodied papionins (primates: Cercopithecinae) inferred from geometric morphometric analysis of landmark data. The Anatomical Record Part A: Discoveries in Molecular, Cellular, and Evolutionary Biology 275, 1048–1072.

Grubb, P., 1999. Evolutionary processes implicit in distribution patterns of modern African mammals. In: Bromage, T.G., Schrenk, F. (Eds.), African Biogeography, Climate Change and Human Evolution. Oxford University Press, New York, pp. 150–164.

Guillot, G., Rousset, F., 2013. Dismantling the Mantel tests. Methods in Ecology and Evolution 4, 336–344.

Hammer, Ø., Harper, D.A.T., 2008. Paleontological Data Analysis. Blackwell, Oxford.

Hill, W.C.O., 1970. Primates: comparative anatomy and taxonomy. In: Cynopithecinae: *Papio*, *Mandrillus*, *Theropithecus*, vol. 8. Edinburgh University Press, Edinburgh, Scotland.

Hoffmann, M., Hilton-Taylor, C., 2008. *Papio ursinus* (errata version published in 2016). The IUCN Red List of Threatened Species 2008: e.T16022A99710253. https://doi.org/10.2305/IUCN.UK.2008.RLTS.T16022A5356469.en (accessed 30.10.17).

IUCN, 2017. The IUCN Red List of Threatened Species. Version 2017-3. http://www.iucnredlist.org/. Downloaded on 30 November 2017.

Jolly, C.J., 1993. Species, subspecies and baboons systematic. In: Kimbel, W.H., Martin, L.B. (Eds.), Species, Species Concepts and Primate Evolution. Springer Science, New York, pp. 67–108.

Jolly, C.J., 2001. A proper study for mankind: analogies from the *Papionin* monkeys and their implications for human evolution. Yearbook of Physical Anthropology 44, 177–204.

Jolly, C.J., 2003. Cranial anatomy and baboon diversity. The Anatomical Record Part A 275, 1043–1047.

Jolly, C.J., Burrell, A.S., Phillips-Conroy, J.E., Bergey, C., Rogers, J., 2011. Kinda baboons (*Papio kindae*) and grayfoot chacma baboons (*P. ursinus griseipes*) hybridize in the Kafue River Valley, Zambia. American Journal of Primatology 73, 291–303.

Keller, C., Roos, C., Groeneveld, L.F., Fischer, J., Zinner, D., 2010. Introgressive hybridization in Southern African baboons shapes patterns of mtDNA variation. American Journal of Physical Anthropology 142, 125–136.

Kingdon, J., 1997. The Kingdon Field Guide to African Mammals. Academic Press, London.

Kingdon, J., Butynski, T.M., De Jong, Y., 2016. *Papio cynocephalus*. The IUCN Red List of Threatened Species 2016: e.T92250442A92250811. https://doi.org/10.2305/IUCN.UK.2016-1.RLTS.T92250442A92250811.en (accessed 30.10.17).

Klingenberg, C.P., 2011. MorphoJ: an integrated software package for geometric morphometrics. Molecular Ecology Resources 11, 353–357.

Klingenberg, C.P., Monteiro, L.R., 2005. Distances and directions in multidimensional shape spaces: implications for morphometric applications. Systematic Biology 54, 678–688.

Klingenberg, C.P., Marugán-Lobón, J., 2013. Evolutionary covariation in geometric morphometric data: analyzing integration, modularity, and allometry in a phylogenetic context. Systematic Biology 62, 591–610.

Kopp, G.H., Ferreira da Silva, M.J., Fischer, J., Brito, J.C., Regnaut, S., Roos, C., Zinner, D., 2014. The influence of social systems on patterns of mitochondrial DNA variation in baboons. International Journal of Primatology 35, 210–225.

Kopp, G.H., Fischer, J., Patzelt, A., Roos, C., Zinner, D., 2015. Population genetic insights into the social organization of Guinea baboons (*Papio papio*): Evidence for female-biased dispersal. American Journal of Primatology 77, 878–889.

Le Boulengé, É., Legendre, P., de le Court, C., Le Boulengé-Nguyen, P., Languy, M., 1996. Microgeographic morphological differentiation in Muskrats. Journal of Mammalogy 77, 684–701.

Legendre, P., Fortin, M.-J., Borcard, D., 2015. Should the Mantel test be used in spatial analysis? Methods in Ecology and Evolution 6, 1239–1247.

Legendre, P., Legendre, L., 1998. Numerical Ecology, 2nd English ed. Elsevier Science BV, Amsterdam, The Netherlands.

Leigh, S.R., 2006. Cranial ontogeny of *Papio* baboons (*Papio hamadryas*). American Journal of Physical Anthropology 130, 71–84.

Leigh, S.R., Cheverud, J.M., 1991. Sexual dimorphism in the baboon facial skeleton. American Journal of Physical Anthropology 84, 193–208.

Matesanz, S., Gimeno, T.E., de la Cruz, M., Escudero, A., Valladares, F., 2011. Competition may explain the fine-scale spatial patterns and genetic structure of two co-occurring plant congeners. Journal of Ecology 99, 838–848.

Mayr, E., 1942. Systematics and the Origin of Species. Columbia University Press, New York.

Mayr, E., 1982. The Growth of Biological Thought: Diversity, Evolution, and Inheritance. Harvard University Press, Cambridge, MA.

McCartney, M., Owen, O., 2007. Technical Note: Hydrology of the Lake Urema Wetland, Mozambique.

McGoogan, K., Kivell, T., Hutchison, M., Young, H., Blanchard, S., Keeth, M., Lehman, S.M., 2007. Phylogenetic diversity and the conservation biogeography of African primates. Journal of Biogeography 34, 1962–1974.

Mitteroecker, P., Bookstein, F., 2011. Linear discrimination, ordination, and the visualization of selection gradients in modern morphometrics. Evolutionary Biology 38, 100–114.

Napier, P.H., 1981. Catalogue of the Primates in the British Museum (Natural History) and Elsewhere in the British Isles. Part II: Family Cercopithecidae, Subfamily Cercopithecinae. British Museum (Natural History), London.

Newman, K.T., Jolly, C.J., Rogers, J., 2004. Mitochondrial phylogeny and systematics of baboons (Papio). American Journal of Physical Anthropology 124, 17–27.

Oksanen, J., Blanchet, F.G., Friendly, M., Kindt, R., Legendre, P., McGlinn, D., Minchin, P.R., O'Hara, R.B., Simpson, G.L., Solymos, P., Stevens, M.H.H., Szoecs, E., Wagner, E., 2018. VEGAN: Community Ecology Package. R package version 2.4-6. https://CRAN.R-project.org/package=vegan.

O'Higgins, P., Collard, M., 2002. Sexual dimorphism and facial growth in papionin monkeys. Journal of Zoology 257, 255–272.

Paradis, E., Claude, J., Strimmer, K., 2004. APE: analyses of phylogenetics and evolution in R language. Bioinformatics 20, 289–290.

Pedersen, C.-E.T., Albrechtsen, A., Etter, P.D., Johnson, E.A., Orlando, L., Chikhi, L., Siegismund, H.R., Heller, R., 2018. A southern African origin and cryptic structure in the highly mobile plains zebra. Nature Ecology & Evolution 2, 491–498.

Phillips-Conroy, J.E., Jolly, C.J., 1986. Changes in the structure of the baboon hybrid zone in the Awash National Park, Ethiopia. American Journal of Physical Anthropology 71, 337–350.

Püschel, T.A., Gladman, J.T., Bobe, R., Sellers, W.I., 2017. The evolution of the platyrrhine talus: A comparative analysis of the phenetic affinities of the Miocene platyrrhines with their modern relatives. Journal of Human Evolution 111, 179–201.

R Core Team, 2017. R: A Language and Environment for Statistical Computing. R Foundation for Statistical Computing, Vienna.

Rightmire, G.P., 2013. Homo erectus and Middle Pleistocene hominins: Brain size, skull form, and species recognition. Journal of Human Evolution 65, 223–252.

Rocha, J.M.L., 2014. The Maternal History of the Sable Antelope (Hippotragus niger) Inferred from the Genomic Analysis of Complete Mitochondrial Sequences. MSc thesis. University of Porto.

Rogers, J., Raveendran, M., Harris, R.A., Mailund, T., Leppälä, K., et al., 2019. The comparative genomics and complex population history of Papio baboons. Science Advances 5, eaau6947.

Samuels, A., Altmann, J., 1986. Immigration and hybridization patterns of yellow and anubis baboons in and around Amboseli, Kenya. International Journal of Primatology 7, 131–138.

Schliep, K.P., 2011. Phangorn: phylogenetic analysis in R. Bioinformatics 27, 592–593.

Slice, D.E., 2001. Landmark coordinates aligned by Procrustes analysis do not lie in Kendall's shape space. Systematic Biology 50, 141–149.

Sholts, S.B., Flores, L., Walker, P.L., Wärmländer, S.K.T.S., 2011. Comparison of coordinate measurement precision of different landmark types on human crania using a 3D laser scanner and a 3D digitiser: Implications for applications of digital morphometrics. International Journal of Osteoarchaeology 21, 535–543.

Singleton, M., 2002. Patterns of cranial shape variation in the Papionini (Primates: Cercopithecinae). Journal of Human Evolution 42, 547–578.

Singleton, M., Seitelman, B.C., Krecioch, J.R., Frost, S.R., 2017. Cranial sexual dimorphism in the Kinda baboon (Papio hamadryas kindae). American Journal of Physical Anthropology 164, 665–678.

Sithaldeen, R., Bishop, J.M., Ackermann, R.R., 2009. Mitochondrial DNA analysis reveals Plio-Pleistocene diversification within the chacma baboon. Molecular Phylogenetics and Evolution 53, 1042–1048.

Sithaldeen, R., Ackermann, R.R., Bishop, J.M., 2015. Pleistocene aridification cycles shaped the contemporary genetic architecture of southern African baboons. PLoS One 10 e0123207.

Stalling, D., Westerhoff, M., Hege, H.C., 2005. Amira: a highly inter-active system for visual data analysis. In: Hansen, C.D., JohnsonC, R. (Eds.), The Visualization Handbook. Elsevier, Amsterdam, pp. 749–767.

Swedell, L., 2011. African papionins: Diversity of social organization and ecological flexibility. In: Campbell, C.J., Fuentes, A., MacKinnon, K.C., Bearder, S.K., Stumpf, R.M. (Eds.), Primates in Perspective, 2nd ed. Oxford University Press, New York, pp. 241–277.

Tinley, K.L., 1977. Framework of the Gorongosa ecosystem Mozambique. PhD dissertation. University of Pretoria.

Vale, C.G., Ferreira da Silva, M.J., Campos, J.C., Torres, J., Brito, J.C., 2015. Applying species distribution modelling to the conservation of an ecologically plastic species (Papio papio) across biogeographic regions in West Africa. Journal for Nature Conservation 27, 26–36.

Vavrek, Matthew J., 2011. Fossil: palaeoecological and palaeogeographical analysis tools. Palaeontologia Electronica 14. http://palaeo-electronica.org/2011_1/238/index.html.

Zinner, D., Groeneveld, L.F., Keller, C., Roos, C., 2009. Mitochondrial phylogeography of baboons (Papio spp.): indication for introgressive hybridization? BMC Evolutionary Biology 9, 83.

Zinner, D., Arnold, M.L., Roos, C., 2011a. The strange blood: natural hybridization in primates. Evolutionary Anthropology 20, 96–103.

Zinner, D., Buba, U., Nash, S., Roos, C., 2011b. Pan-African Voyagers: The phylogeography of baboons. In: Sommer, V., Ross, C. (Eds.), Primates of Gashaka: Socioecology and Conservation in Nigeria's Biodiversity Hotspot. Springer New York, New York, NY, pp. 319–358.

Zinner, D., Keller, C., Nyahongo, J.W., Butynski, T.M., Jong, Y.A. de, Pozzi, L., Knauf, S., Liedigk, R., Roos, C., 2015. Distribution of mitochondrial clades and morphotypes of baboons Papio spp. (Primates: Cercopithecidae) in Eastern Africa. Journal of East African Natural History 104, 143–168.

Zinner, D., Wertheimer, J., Liedigk, R., Groeneveld, L.F., Roos, C., 2013. Baboon Phylogeny as inferred from complete mitochondrial genomes. American Journal of Physical Anthropology 150, 133–140.